CMU Journal of Science
The Official Scientific Journal of Central Mindanao University
ISSN Print: 0116-7847 js.cmu.edu.ph ISSN Online: 2704-3703

Research Article

Assessing Liquefaction Potential Using Liquefaction Potential Index (LPI) and Ground-Response Analysis –Based on PSHA-Based Ground Motions

Carmina B. Borja*, Richelle G. Zafra, Perlie P. Velasco, Marish S. Madlangbayan

Department of Civil Engineering, College of Engineering and Agro-Industrial Technology, University of the Philippines Los Baños, Laguna, Philippines

* Correspondence: cbborja1@up.edu.ph (C.B.B.)

ABSTRACT

Liquefaction potential index (LPI) is an empirical parameter that predicts the surface manifestation of liquefaction. In this study, the result of LPI for two cities (Calamba and Cabuyao) of Laguna was evaluated due to historical liquefaction occurrences attributed to earthquake events and volcanic eruptions. These sites represented liquefiable and a non-liquefiable case. LPI was validated through site-specific ground response analysis (GRA) using a nonlinear soil model and using input motions based on the probabilistic approach. Using SPT data from 22 locations, result of LPI reveals that the borehole sites in Cabuyao City have a low to very high liquefaction potential, while in Calamba City, the sites have a moderate to very high liquefaction potential. The high potential for liquefaction in Calamba was affirmed through ground response analysis. Further verification with empirical data is recommended to determine the applicability and limitations of the procedure.

Keywords: Liquefaction Potential Index, Ground Response Analysis, Probabilistic Seismic Hazard Analysis

Citation: Borja, C.B., Zafra, R.G., Velasco, P.P., Madlangbayan, M.S. (2025). "Assessing Liquefaction Potential Index (LPI) and Ground-Response Analysis-Based on PSHA-Based Ground Motions." CMU Journal of Science. 29(1). 51

Academic Editor: Dr. Ma. Bernadeth Lim

Received: May 20, 2025
Revised: June 11, 2025
Accepted: June 24, 2025
Published: July 25, 2025

1. INTRODUCTION

Liquefaction is a phenomenon wherein soil materials behave like liquid due to increased pore water pressure, making the soil weaker or unable to support loads like buildings. Soils have a natural tendency to densify when shaken, forming a more consolidated soil orientation and prohibiting water drainage. If the soil is saturated and an undrained condition occurs during the shaking, the pore water pressure rises. Once the pore water pressure increases to an amount equal to the pressure exerted by the soil above it, liquefaction will occur. This generally happens in loose and cohesionless soil [1]. In the Philippines, liquefaction was brought into public awareness during the 16th July 1990 earthquake when extensive liquefaction occurred in the provinces of Tarlac, Pangasinan, and La Union [2]. Buildings, road networks, bridges, and pipelines located in coastal areas are at risk of being affected by liquefaction hazards [3].

Liquefaction and the accompanying effects commonly occur at sites with particular geologic conditions and level of seismicity [4]. Soils at certain sites are more prone to liquefy than others based on their geologic and geotechnical characteristics. This is referred to as liquefaction susceptibility [1].

In addition to liquefaction susceptibility, another requisite for liquefaction occurrence is the seismic condition that favors the production of ground failure, termed as liquefaction opportunity. This is closely related to the seismic hazard in a certain area. Liquefaction opportunity is dependent on the rate of occurrence of earthquakes that produce certain levels of ground shaking enough to trigger liquefaction in susceptible soils, and on the proximity of a certain area to the earthquake source [5]. To quantify the level of ground shaking, ground motions produced by earthquakes are commonly described in terms of amplitude parameters, frequency content, and duration [1].

The combined effects of liquefaction susceptibility and liquefaction opportunity are captured in the term liquefaction potential [5].

Liquefaction potential index (LPI) was developed by Iwasaki et al. in 1978 to predict the surface manifestation of liquefaction. This parameter was originally formulated using SPT data from liquefied and non-liquefied sites in Japan. Unlike the Simplified Procedure that evaluates liquefaction potential for only a certain soil element, LPI may be used to evaluate liquefaction potential for a soil column up to a depth of 20m. The limiting depth of 20m was chosen because surface manifestation seldom happens when liquefaction occurs at depths greater than 20m [6].

Seismic hazard analysis approach for ground shaking and liquefaction can be either deterministic or probabilistic [1]. The deterministic approach considers the maximum earthquake magnitude that may occur on a specific fault. It is used in places where buildings are near major active faults. On the contrary, the probabilistic approach considers the likelihood of the occurrence of all the earthquakes at different sources. This approach is especially useful for mapping purposes [6].

Probabilistic seismic hazard analysis (PSHA) is a process of obtaining a hazard curve, which gives information on the likelihood that a parameter describing a ground motion is equaled or exceeded in terms of mean annual probability [7]. Spectral acceleration and PGA values may also be derived from this method. Moreover, PSHA allows the generation of time histories for use in ground response analysis [8]. The seismic hazard curves and the spectral acceleration values used in this study were obtained from the PSHA conducted for Laguna, Philippines, by Aguirre (2013) [9].

Studies on the determination of LPI verified using probabilistic-based nonlinear ground response analysis is limited. Mase et al. (2020) [10] conducted numerical and empirical analyses to quantify liquefaction potential index in Bengkulu City, Indonesia using bore log information and shear velocity profiles. Similarly, Mitra et al. (2021) [11] conducted ground response analysis to obtain PGA values for use in the LPI computation, to assess the liquefaction potential in a site in Kolkata, West Bengal, India. Adampira et al. (2015) [12] performed one-dimensional ground response analysis to determine site response due to near-fault earthquakes for a liquefiable project site in Iran. Kumar et al. (2023) [13] determined the liquefaction potential in Kolkata, India, using numerical analyses (equivalent linear and nonlinear) and the simplified method. All these mentioned studies conducted ground response analysis using input motions based on the deterministic approach.

In this study, probabilistic seismic hazard analysis is used to set the criteria for selecting the input ground motions for ground response analysis. LPI based on a simplified procedure was computed, and its results were verified using ground response analysis. This highlights the use of ground response analysis to validate the results of evaluation procedures in cases where there are scant case histories, wherein comparison can be made.

2. METHODOLOGY

The methodology consists of three major parts: classification of the site based on borehole information, computation of liquefaction potential index, and verification through site-specific ground response analysis.

In this study, liquefaction potential was evaluated for the two cities (Calamba and Cabuyao) of Laguna, one of the top provincial contributors to the Philippines' gross domestic product [14], located south of the National Capital Region. Laguna has had historical liquefaction occurrences attributed to earthquake events and volcanic eruptions [3]. This information is important because liquefaction tends to recur at the same location based on post-earthquake field investigations [1] (p. 352).

Calamba and Cabuyao were chosen as the sites of interest for evaluation of liquefaction potential because of four main reasons: 1) the proximity of the cities to Laguna Lake and the presence of rivers and tributaries within the area create a saturated environment for the soils; 2) the geology in the area being underlain with young river deposits especially at the shorelines allows the formation of weak soils; 3) the seismicity in the area creates an opportunity for liquefaction (because the sites are within the 150km-radius from active faults such as the Philippine Fault: Infanta Segment and the Valley Fault System); 4) the urbanization and the industrialization in the area increase the risk of loss, both in terms of lives and damages; and, 5) the availability of borehole data.

2.1. Site Classification

This study used the site classification and corresponding site factors for spectral acceleration in the AASHTO LRFD Bridge Design Specifications 2012. While the local code has its own site classification based on American standards, this standard is referred in this study in the absence of provisions for site response analysis in the local code. Site classes may be any of the six: Site Class A (hard rock), Site Class B, Site Class C, Site Class D, Site Class E, and Site Class F, arranged from the best to problematic soils. The criteria for identifying the site classification of an area that depends on either the shear wave velocity (Vs), the average SPT blowcount ($\overline{N}$), or the undrained shear strength.

Since the peak ground acceleration produced in PSHA is derived for a base rock, the PGA measured should be corrected in accordance to the site classification of the borehole location ($PGA_{corrected}$). For this study, SPT-N values were used to compute the average standard penetration resistance for the top 100 ft, denoted by $\overline{N}$. The value of $\overline{N}$ is computed using Equation 1 FROM NSCP 2015 [15]:

$$\overline{N} = \frac{\sum_{i=1}^{n} d_i}{\sum_{i=1}^{n} \frac{d_i}{N_i}} \quad \text{(Equation 1)}$$

where N_i = SPT-N measured directly from the field, uncorrected blow count of the "*ith*" layer not to exceed 100ft ≈ 30m; d_i = thickness of the "*ith*" layer (ft).

The SPT-N measured at the last layer in each profile was assumed for depths up to 100 ft in this study. This study uses the correction factors for PGA from AASHTO (2012) [16]. Intermediate values are computed by linear interpolation.

The SPT-N values were obtained from soil investigation reports obtained from the Engineering Offices of Cabuyao City and Calamba City. A total of 22 borehole sites were identified, 14 in Calamba and 8 in Cabuyao. Each borehole site consisted of one to three borehole logs. The depth of the collected soil profiles varied from 9 to 15m. The reports included information on the location of boreholes in the site, standard penetration test number (SPT-N), description of soil layers, Atterberg limits (liquid limit and plasticity index), location of ground water table from the surface (GWT), and sieve analysis. Most reports also contain suggested/actual values of effective unit weight. Figure 1 shows the locations of borehole sites in Cabuyao and Calamba.

2.2. Liquefaction Potential Index

LPI was computed using Equation 2 based Iwasaki et al. (1982) [17]. The equation was developed under the assumption that the extent by which liquefaction may be damaging is proportional to the thickness of liquefiable layers, the nearness of the liquefiable layers to the ground surface, and the deviation of the factor of safety from the threshold value. The variable *F* is a function of the factor of safety (*FS*), quantifying the amount by which FS is less than 1. On the other hand, the weighting factor is influenced by the depth of the soil layer. It has a minimum value (*F* = 0) at the ground surface and a maximum value at the bottom layer of the soil column [6]. LPI may have a maximum value of 100 for sites with very high liquefaction potential.

$$LPI = \int_0^{20m} Fw(z)dz \quad \text{(Equation 2)}$$

where:

F = 1−*FS*, for *FS* < 1; and *F* = 0, for *FS* > 1

w(z) = weighting factor = 10−0.5*z*

z = depth in meters

Luna and Frost (1998) (as cited by Dixit, Dewaikar & Jangid 2011) [18] used a different relation to compute for the LPI of profiles with less than 20m of depth, as shown in Equation 3:

$LPI = \sum_{i=1}^{n} w_i F_i H_i$ (Equation 3)

F_i = 1−FS_i for FS_i < 1.0 (Equation 3-a)

F_i = 0 for FS_i > 1.0 (Equation 3-b)

where:

H_i = thickness of the discretized soil layers

n = number of layers

F_i = liquefaction severity for *i*-th layer

FS_i = factor of safety for *i*-th layer

w_i = weighting factor =10–0.5 z_i

z_i = the depth of *i*-th layer (m)

Sonmez (2003) [19] gave a more conservative modification of the threshold value of Iwasaki et al. (1982) by increasing the factor of safety to 1.2. Equation 4-a, Equation 4-b, and Equation 4-c the proposed computation for F [19]. He also categorized the level of liquefaction potential based on the values of *LPI*. An *LPI* = 0 indicates sites where liquefaction is not likely to happen; 0 < *LPI* < 2 indicates low liquefaction potential; 2 ≤ *LPI* ≤ 5 indicates moderate liquefaction; 5 < *LPI* < 15 indicates high liquefaction potential; and, *LPI* > 15 indicates very high liquefaction potential.

$F = 0 \quad for \quad FS \geq 1.2$ (Equation 4-a)

$F = 1 \quad for \quad FS \leq 0.95$ (Equation 4-b)

$F = 2 \times 10^{6} e^{-18.427FS} \quad for \quad 1.2 > FS > 0.95$ (Equation 4-c)

The use of LPI is advantageous in that it gives a concrete idea on the liquefaction effects that may be expected to occur. However, since LPI is an empirical parameter and was derived from specific tectonic setting that may be different from what is present at the site of interest, validation of the results must be done, for example, using field case liquefaction histories.

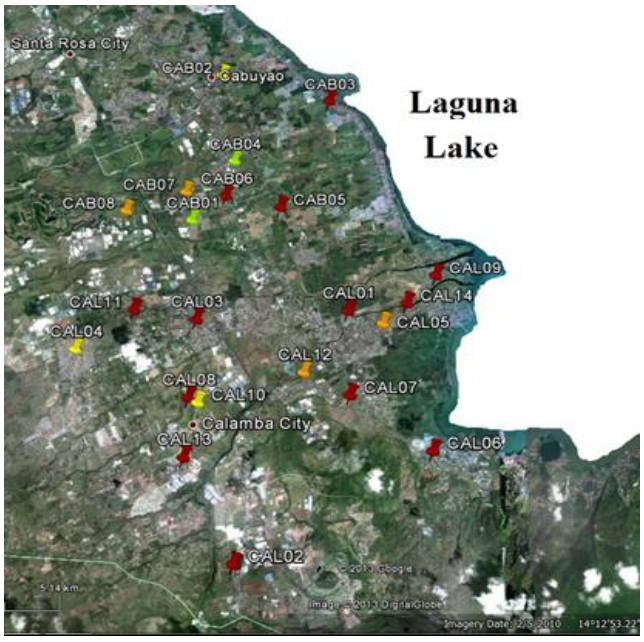

Figure 1. Borehole locations in Cabuyao and Calamba

2.3. Site-Specific Ground Response Analysis

In the absence or sparseness of strong ground motion recording for a particular area of interest, simulated earthquake motions may be used [8]. Related to this is the technique called ground response analysis. Ground response analysis is used in predicting ground surface motions, evaluating liquefaction potential, and determining seismic-related loading that may cause instability of earth and earth-retaining structures [1]. The term ground response refers to the effects of rock and soil condition on the propagation of seismic waves near the earth surface [8].

Ideally, ground response analysis involves modeling of three processes: the release of strain energy from the earthquake source, the travel of seismic waves from the earthquake source through the bedrock, and the propagation of waves from the bedrock to the ground surface. However, modeling the first two processes is too complicated that it becomes impractical to incorporate them in common engineering applications [1]. Thus, only the last process remains addressed. In addition, recognizing that soil conditions vary locally, the term 'site-specific' is affixed.

In ground response analysis, one of the important aspects is setting an input motion to simulate an earthquake at a site. This may be done by obtaining time histories of several recorded earthquakes measured in two horizontal components. In the local code, ground motion must be taken for an earthquake event with a minimum of 10% probability of being exceeded in 50 years, which corresponds to a 475-yr return period, and which takes into account the geologic, tectonic, seismologic, and soil characteristics of the site [15].

Moreover, in the selection of time history, seismic hazard must be deaggregated [8]. Deaggregation or disaggregation is the process of obtaining the most critical ranges of magnitude and source-to-site distances having the highest contribution to hazard at a specific site [20]. In this study, deaggregation was done using MATLAB codes and using the results of PSHA. The magnitude-distance combination was deaggregated for PGA, peak spectral accelerations at 0.2 second and 1 second; these are arbitrarily chosen to account for the short-period and long-period structures in the area.

Once selected, the response spectra of these time histories must match the target spectrum site (i.e., the design spectrum of the site of interest) in the process called spectral matching, since seismological characteristics of records affect the shape of the response spectrum [21]. Spectral matching is done by modifying the frequency content of the ground motion record to match the target spectrum at all spectral periods [22]. This technique ensures that ground motions similar to actual earthquake are simulated at the site of interest so that the effect of varying responses of structure and/or soil condition is reduced, if not eliminated. It makes analyses more practical since there is no need to simulate using a very large number of real earthquake records [23].

A spectral matching software called RSPMatchEDT [24] was used in this study. By inputting the coordinates of the target spectrum and the coordinates of the accelerogram record (i.e., the time history for acceleration) of the earthquake, the time history of the spectrally matched records is produced. Spectral matching was done using seven earthquakes and six earthquakes (in two components) for the liquefied and non-liquefied case, respectively.

Boundary conditions may be elastic or rigid. In a rigid boundary, once the seismic waves pass through the bedrock, the energy becomes trapped in the overlying soils; as a result, the waves continuously bounce back and forth from the bedrock to the soil layer. An elastic boundary condition, on the other hand, represents a relatively soft bedrock. In this type of boundary condition, energy is dissipated. Furthermore, only a part of the downward-traveling seismic waves is partially reflected in the overlying soil; the other waves will travel below the bedrock until energy is completely dissipated within the soil layer [1]. An elastic boundary condition is considered in this study because it is more realistic than a rigid boundary given the relatively young geologic deposits in the Philippines.

Soil, as a material, is known to be nonlinear and hysteretic (i.e., the stress-strain diagram curve of soil follows a different path every time it is unloaded and reloaded). This is primarily attributed to damping. A portion of the elastic energy is converted to heat, resulting in a decrease in the amplitude of a traveling wave [1]. Thus, this study used a nonlinear approach – the soil column is discretized into smaller layers. The soil and material properties of the layers were defined using the information from the soil investigation reports. The response of individual layers in each time domain is computed using numerical integration techniques; by doing so, the stress-strain relationship may be analyzed linearly but in very small-time steps [1].

The ground response analysis performed used a one-dimensional model, wherein waves are propagated vertically from the base rock to the ground surface, and the analysis used the nonlinear solution. This model assumes

that only horizontal boundaries exist. This means that the layers of soil and the bedrock stretch infinitely in the horizontal directions, and that the traveling waves are predominantly SH-waves. Analyses based on these assumptions are found to agree with the measured response for many cases [1], and they have been applied in previous studies that conducted seismic ground response analysis [10,11]. Also, a permeable bottom layer was used to simulate pore water pressure dissipation that exists in the natural condition. Simulation was performed using DEEPSOIL v5.1 [25]. In the software, the soil profile for the site of interest is defined using the geotechnical information (e.g., thickness and depth of layer, unit weight, plasticity index, etc.) from the soil investigation report. Standard curves proposed by Vucetic and Dobry (1991) [26] for clay and Seed and Idriss (1970) [27] for sand are used to define the material behavior, as in Mitra et al. (2021) [11] wherein there are no available site-specific modulus reduction and damping ratio curves. The uniform hazard curve of the site and the time history of the matched earthquake record are the inputs. The results of the simulation are in the form of stress-strain curves and pore water accumulation ratio plots in each layer, and strain and pore water pressure profiles that are used in the evaluation of liquefaction.

3. RESULTS AND DISCUSSION

3.1 Site Classification and Liquefaction Potential Index

Using a total of 39 borehole logs representing 22 borehole sites, the liquefaction potential indices at specific sites in Cabuyao City and Calamba City were determined. Table 1 summarizes the LPI computed for the borehole sites in Cabuyao City, where all the borehole sites were identified as Site Class D. On the other hand, Table 2 summarizes the LPI values for Calamba City, where the borehole sites were either Site Class D or Site Class E. The average LPI (LPI_{AVE}) in Cabuyao ranges from 0 to 26 indicating low to very high liquefaction potential. In Calamba, the average LPI values range from 3 to 47, indicating moderate to very high liquefaction potential. It is also notable that 9 of the 14 borehole sites in Calamba have very high liquefaction potential.

Table 1. Liquefaction potential for the borehole sites in Cabuyao City

Borehole ID	Latitude, Longitude	GWT	Nave	Site Class	$PGA_{corrected}$ (in g)	LPI_{AVE}
CAB01	14°14'11.15"N, 121° 7'17.48"E	15 15	49 50	D	0.378	0
CAB02	14°16'36.62"N, 121° 7'36.63"E	3 3	29 36	D	0.381	4
CAB03	14°16'10.65"N, 121° 9'13.65"E	1.22 0.9	27 27	D	0.376	19
CAB04	14°15'10.45"N, 121° 7'50.85"E	4 4	50 50	D	0.378	0
CAB05	14°14'26.13"N, 121° 8'32.87"E	3 3	23 21	D	0.375	26
CAB06	14°14'36.91"N, 121° 7'9.75"E	1.85 1.85 1.85	20 16 22	D	0.378	25
CAB07	14°14'40.20"N, 121° 7'9.75"E	NR NR NR	31 31 31	D	0.379	7
CAB08	14°14'20.74"N, 121° 6'19.39"E	3 2	26 26	D	0.381	9

Notes: N_{ave} – average SPT-N values of boreholes based on the borehole investigation report; NR – not reached

Table 2. Liquefaction potential for the borehole sites in Calamba City

Borehole ID	Latitude, Longitude	GWT	N_{ave}	Site Class	$PGA_{corrected}$ (in g)	LPI_{AVE}
CAL01	14°12'48.48"N, 121° 9'33.43"E	1.5	14	E	0.363	47
CAL02	14° 9'15.19"N, 121° 8'5.68"E	1.5	16	D	0.366	39
CAL03	14°12'40.10"N, 121° 7'25.82"E	1.5	41	D	0.374	26
CAL04	14°12'12.84"N, 121° 5'46.63"E	8.1 5.2	28 50	D	0.378	5
CAL05	14°12'37.14"N, 121°10'2.90"E	1.18 1.18	30 19	D	0.367	13
CAL06	14°10'47.47"N, 121°10'43.57"E	1.5	16	D	0.364	40
CAL07	14°11'34.20"N, 121° 9'35.90"E	NR NR	16 17	D	0.395	11
CAL08	14°11'31.50"N, 121° 7'22.73"E	1.67 2.05	50 50	D	0.372	38
CAL09	14°13'20.83"N, 121°10'47.59"E	3.6 5.2	23 17	D	0.362	21
CAL10	14°11'27.38"N, 121° 7'30.76"E	4.6 4.1	34 37	D	0.372	3
CAL11	14°12'48.48"N, 121° 6'32.98"E	1.5	28	D	0.377	27
CAL12	14°11'53.67"N, 121° 8'57.36"E	3 3	41 25	D	0.369	8
CAL13	14°10'41.03"N, 121° 7'21.49"E	1.5	27	D	0.371	26
CAL14	14°12'55.53"N, 121°10'22.71"E	1.5	13	E	0.362	46

Notes: N_{ave} – depth of groundwater table and average SPT-N values of boreholes based on the borehole investigation report; NR – not reached

3.2 Site-Specific Ground Response Analysis

3.2.1 Deaggregation

Deaggregation of the sites indicates that an earthquake with a moment magnitude of around 7.2 occurring in the nearest 44 km from the site has the highest contribution of hazard in the area. Figure A1, Figure A2, and Figure A3 show the result of the deaggregation for PGA, and spectral accelerations at T=0.2 sec and T=1 sec at a 475-yr return period earthquake event, respectively.

The results of the deaggregation, which forms the basis for the selected ground motions to be used for ground response analysis can be found in Appendix A.

3.2.2 Analysis results in DEEPSOIL v5.1

The Banadero borehole site (CAL01 in Figure 1) in Calamba, having the highest LPI among the others, was evaluated using a site-specific ground response analysis. Seven earthquakes, with a magnitude range of 6.8 to 7.5, were simulated in the ground response analysis. All earthquake events resulted to the occurrence of liquefaction at the layer located around 4 m from the surface, where porewater pressure accumulation was observed. In this layer, the ratio of the porewater pressure to the effective vertical stress is almost equal to one, signaling the occurrence of liquefaction. Similarly, ground response analysis was performed for Banay-Banay, Cabuyao, (CAB04 in Figure 1) which yielded a value of LPI = 0. Six earthquakes, with a magnitude range of 6.8 to 7.6, were simulated in the ground response analysis. Generally, relatively small strains were produced in the simulation and pore water did not accumulate. However, liquefaction occurred for the earthquake with a magnitude of 7.6. strain in the soil layer at a depth of 13.5m (Layer 11) reached 6% as shown in Figure 2. At a depth of around 13.5m,

porewater accumulation was observed, and the ratio of the porewater pressure to the effective vertical stress is almost equal to one as shown in Figure 3. For this borehole site, the prediction of ground response analysis is different with prediction based on LPI. The findings align with those of Kumar et al. (2023) [28], demonstrating that the simplified method was inadequate in predicting the liquefaction susceptibility of the site. Instead, susceptibility was effectively assessed through equivalent-linear and nonlinear ground response analyses.

The porewater pressure profiles for the sites are presented in Appendix B.

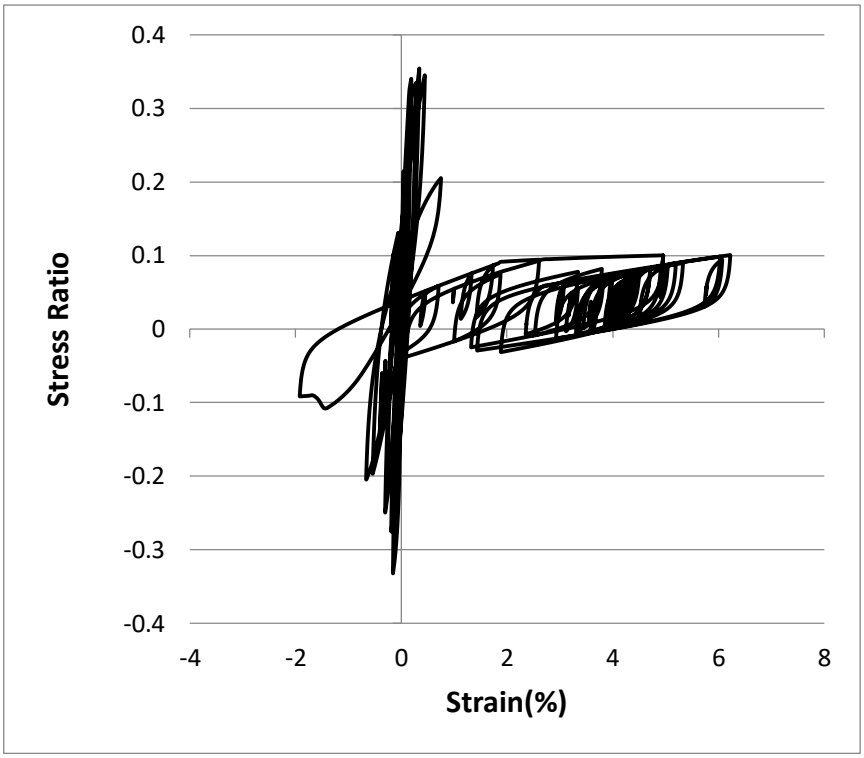

Figure 2. Stress-strain curve of Layer 11 in the Banay-Banay site for the magnitude 7.6-earthquake

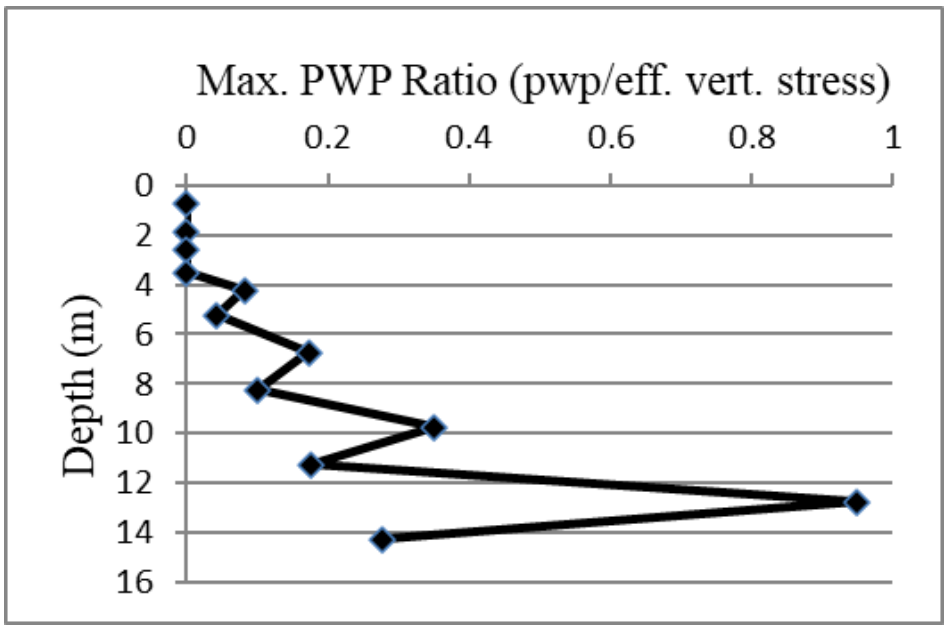

Figure 3. Pore water pressure ratio for the Banay-Banay site generated by a magnitude 7.6 earthquake

4. CONCLUSION

This study demonstrated how PSHA results can be used as a tool for the evaluation of liquefaction. This was done in two ways: by directly getting peak ground acceleration from PSHA results for use in the computation of liquefaction potential index, and by obtaining time histories for ground response analysis in order to verify liquefaction or nonliquefaction of soils in cases where there is no recorded liquefaction. Furthermore, the use of nonlinear soil model with pore water pressure dissipation enabled a detailed analysis on the behavior of soils during seismic loading. The result of LPI reveals that the borehole sites in Cabuyao City have a low to very high liquefaction potential, while in Calamba City, the sites have a moderate to very high liquefaction potential. The high potential for liquefaction in the Banadero site was affirmed through ground response analysis. However, the ground response analysis done in Banay-Banay shows that the site is not completely non-liquefiable but may liquefy for earthquake events with at least a magnitude of 7.6. The use of LPI in the evaluation of liquefaction potential is recommended to be further verified with available empirical evidence to determine the applicability and limitations of this procedure.

Author Contributions: XXX: Conceptualization, Data collection and analysis, Manuscript Writing. XXX: Supervision, Writing – Review and Editing. XXX – Review and Editing. XXX: Writing – Review and Editing.

Funding: There is no external funding given for this research.

Data Availability Statement: Data used for analysis are not available for public access. An agreement was made with the Engineering Office of Calamba City and the Engineering Office of Cabuyao City to utilize the data for research purposes only. However, a written request may be given to the authors, subject to approval.

Acknowledgments: The researchers would like to thank the Engineering Office of Calamba City and the Engineering Office of Cabuyao City for providing the borehole data, and the Mines and Geosciences Bureau for providing the geologic map used in this study. The researchers would also like to thank of Vibrametrics, Inc., for sharing his expert guidance; of PHIVOLCS Geology & Geophysics R&D Division, for sharing her knowledge on liquefaction; and, the whole staff of the PHIVOLCS library for their generous assistance during the research visits. Without the support and data provided, this study would not have been completed.

Conflicts of Interest: The authors declare no conflict of interest for this research.

5. REFERENCES

AASHTO LRFD bridge design specifications. 2012. Washington, D.C.: American Association of State Highway and Transportation Officials.

Adampira, M., Alielahi, H., Panji, M., & Koohsari, H. 2015. Comparison of equivalent linear and nonlinear methods in seismic analysis of liquefiable site response due to near-fault incident waves: a case study. Arabian Journal of Geosciences, 8(5), 3103–3118. Doi: 10.1007/s12517-014-1399-6

Aguirre, J. J. 2013. Probabilistic seismic hazard analysis of Laguna, Philippines. [unpublished thesis]

Al Atik, L., & Abrahamson, N. 2010. An Improved Method for Nonstationary Spectral Matching. *Earthquake Spectra, 26(3)*, 601–617. DOI: 10.1193/1.3459159

Anderson, J. G. 2003. Strong-motion seismology; Lee, W. H. K., Kanamori, H., Jennings, P. C. & Kisslinger, C. (Eds.). In International Handbook of Earthquake Engineering and Seismology Part B, London: Academic Press.

Association of Structural Engineers of the Philippines, Inc. (ASEP). 2016. National Structural Code of the Philippines, 2015. Volume 1, Buildings, towers, and other vertical structures.

Bazurro, P., and Cornell, C.A. 1999. Disaggregation of Seismic Hazard. *Bulletin of the Seismological Society of America, 89 (2)*, 501-520.

Buhay, D. J. L., Legaspi, C. J. M., Dizon, R. P. A., Abigania, M. I. T., Papiona, K. L., & Bautista, M. L. P. 2024. Development of a database of historical liquefaction occurrences in the Philippines. *Earth-Science Reviews, 251*, 104733. DOI: 10.1016/j.earscirev.2024.104733

CALABARZON. 2024. Laguna's economy posted 3.9 percent growth in 2023. Press release on 2023 provincial product accounts. https://rsso04a.psa.gov.ph/content/lagunas-economy-posted-39-percent-growth-2023

Dixit, J., Dewaikar, D. M., and Jangid, R. S. 2012. Assessment of liquefaction potential index for Mumbai city. *Nat. Hazards Earth Syst. Sci., 12*, 2759–2768. DOI: 10.5194/nhess-12-2759-2012.

Grant, D.N., Greening, P.D., Taylor, M.L., and Ghosh, B. 2008. Seed record selection for spectral matching with RSPMatch2005. In the Proceedings of the 14th

World Conference on Earthquake Engineering, Beijing, China, October 12-17.

Hancock, J. Bommer, J.J., and Stafford, P.J. 2008. Numbers of Hashash, Y.M.A., Musgrove, M.I., Harmon, J.A., Ilhan, O., Groholski, D.R., Phillips, C.A., and Park, D. 2017. DEEPSOIL 7.0, User Manual.Holzer, T.L. 2012. Probabilistic liquefaction hazard mapping. In the Proceedings of Geotechnical Earthquake Engineering and Soil Dynamics IV. DOI: 10.1061/40975(318)30

Holzer, T.L. 2012. Probabilistic liquefaction hazard mapping. In the Proceedings of geotechnical earthquake engineering and soil dynamics IV, Sacramento, CA, 1-32. DOI: 10.1061/40975(318)30.

Iwasaki, T., Arakawa, T., and Tokida, K. 1982. Simplified procedures for assessing soil liquefaction during earthquakes. In the Proceedings of the Conference on Soil Dynamics and Earthquake Engineering, Southampton, UK, 925-939.

Kramer, S.L. Geotechnical earthquake engineering, In: Prentice-Hall international series in civil engineering and engineering mechanics. Prentice-Hall New Jersey, U.S.A., 1996; pp. 348-419.

Kumar, S., Muley, P. & Madani, S.N. 2023. Ground response analysis and liquefaction for Kalyani region, Kolkata. *Environ Sci Pollut Res 30,* 99127–99146. DOI: 10.1007/s11356-022-23680-8 Philippine Statistics Authority Region IVA –

Kumar, S., Srivastav, T., Muley, P. 2021. Assessment of SPT-Based Liquefaction Potential of Kalyani Region, Kolkata; Patel, S., Solanki, C.H., Reddy, K.R., Shukla, S.K. (eds). In the Proceedings of the Indian Geotechnical Conference 2019, Lecture Notes in Civil Engineering, vol 138. Springer, Singapore. DOI: 10.1007/978-981-33-6564-3_22

Mase, L. Z., Farid, M., Sugianto, N., & Agustina, S. 2020. The Implementation of Ground Response Analysis to Quantify Liquefaction Potential Index (LPI) in Bengkulu City, Indonesia. *Journal of the Civil Engineering Forum, 6(3)*, 319-329. DOI: 10.22146/jcef.57466

Mitra, T., Chattopadhyay, K. K., & Ghosh, A. 2021. Ground Response Analysis and Determination of Liquefaction Potential Index; M. Latha Gali & P. Raghuveer Rao (Eds.). *Geohazards: Proceedings of IGC 2018,* 345–352. DOI: 10.1007/978-981-15-6233-4_24

Murayama, Y., & Hirano, S. 1993. The damage and the rehabilitation process after 1990 Luzon Earthquake – Some cases of La Union and Nueva Ecija. The Science Reports of the Tohoku University, 7th Series (Geography), 43(1), 27-48.

Ordonez, G.A. (2012) RSPMatchEDT – A Pre-Processor and Post-Processor for RspMatch2005 & RspMatch2009. GeoMotions, LLC; Lacey, Washington, USA.

scaled and matched accelerograms required for inelastic dynamic analyses. *Earthquake Engng Struct. Dyn., 37*, 1585-1607. DOI: 10.1002/eqe.827

Seed H.B., and Idriss I.M. 1970. Soil moduli and damping factors for dynamic response analyses. Report EERC, pp 70–10. Earthquake Engineering Research Centre, University of California, Berkeley

Sonmez, H. Modification of the liquefaction potential index and liquefaction susceptibility mapping for a liquefaction-prone area (Inegol,Turkey). *Env Geol* , 2003, 862–871 (2003). DOI: 10.1007/s00254-003-0831-0

Stewart, J. P., Chiou, S., Bray, J. D., Graves, R. W., Somerville, P. G., and Abrahamson, N. A. 2001. Ground Motion Evaluation Procedures for Performance-Based Design, PEER Report 2001-09. Pacific Earthquake Engineering Research Center, University of California, Berkeley, CA.

Vucetic, M., and Dobry, R. 1991. Effect of soil plasticity on cyclic response. *J Geotech Eng Div ASCE 117(1),* 89–107. DOI: 10.1061/(ASCE)0733-9410(1991)117:1(89)

Youd, T. L. 2003. 70 Liquefaction mechanisms and induced ground failure. In International Geophysics, 81, 1159–1173, Elsevier. DOI: 10.1016/S0074-6142(03)80184-5

Youd, T. L., and Perkins, D. M. 1978. Mapping liquefaction-induced ground failure potential. *Journal of the Geotechnical Engineering Division, 104(4)*, 433-446. DOI:10.1061/AJGEB6.0000612

Appendix A: Ground Motions for Ground Response Analysis

A.1 Seismic Hazard Deaggregation

This section contains the result of the deaggregation, selection of ground motion records, spectral matching, and ground response analysis.

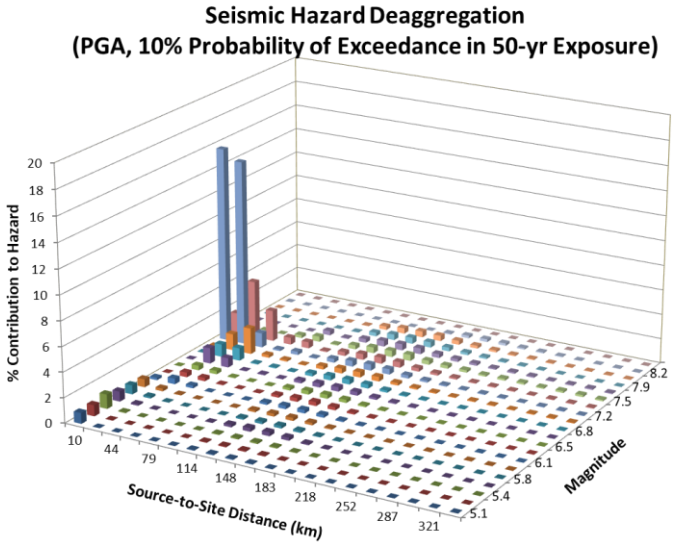

Figure A1. Seismic hazard deaggregation for PGA at a 475-yr return period earthquake event

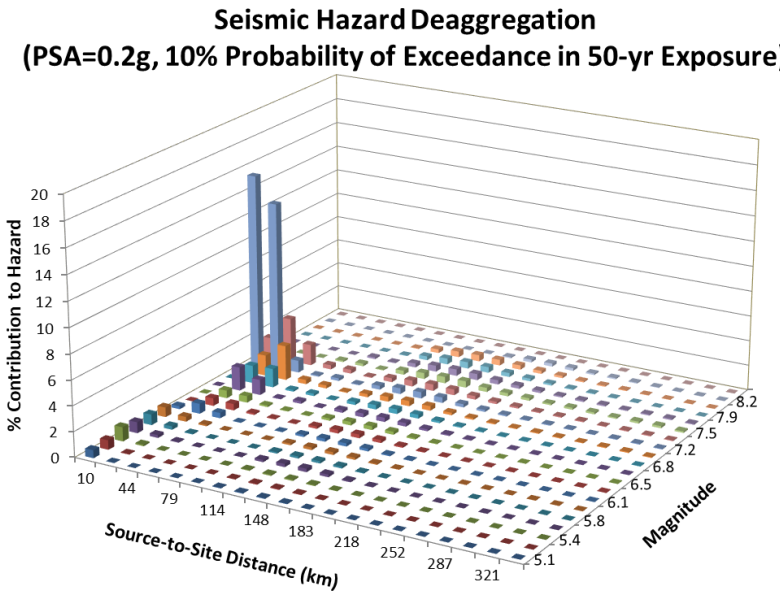

Figure A2. Seismic hazard deaggregation for PSA at 0.2 sec at a 475-yr return period earthquake event

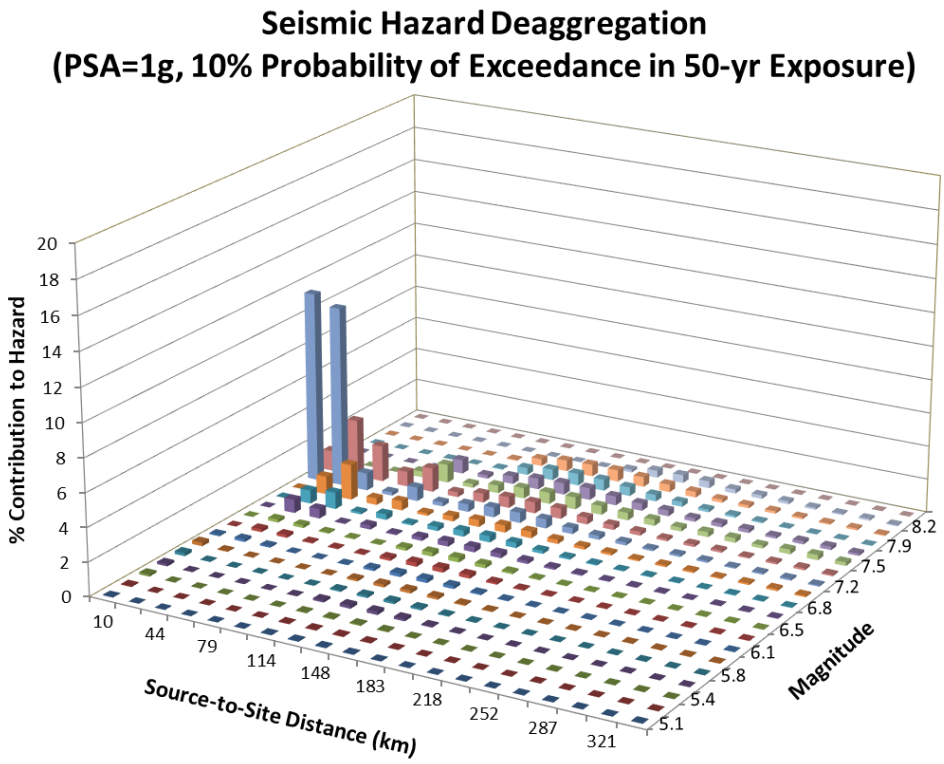

Figure A3. Seismic hazard deaggregation for PSA at 1 sec at a 475-yr return period earthquake event

A.2 Selected earthquake records for simulation

Table A1. Selected earthquake records for the Banaderos site

Description of Event	Magnitude	Distance to Station (km)	Fault Mechanism	Recorded PGA (in g)	
				x	y
EQ1: DUZCE, TURKEY 1999 p Stn: Duzce	7.1	6.6	Strike-Slip	0.31	0.54
EQ2: KOBE, JAPAN 1995 p Stn: MZH Station	6.9	70.3	Strike-Slip	0.06	0.05
EQ3: KOCAELI, TURKEY 1999 p Stn: Arcelik	7.5	10.6	Strike-Slip	0.22	0.15
EQ4: HECTOR MINE 1999 c Stn: Joshua Tree Fire Station	7.1	51.5	Strike-Slip	0.15	0.19
EQ5:LANDERS 1992 c Stn: Palm Springs - Airport	7.4	41.9	Strike-Slip	0.08	0.09
EQ6: WHITTIER NARROWS p Stn: Alhambra, Fremont	6	11.8	Reverse Oblique	0.3	0.25
EQ7: BORREGO MOUNTAIN 1968 c Stn: USGS Station 117	6.8	34.7	Strike-Slip	0.13	0.06

Note: Stn – Station where the ground motion was recorded

Table A2. Selected earthquake records for the Banay-Banay site

Description of Event	Magnitude	Distance to Station (km)	Fault Mechanism	Recorded PGA (in g)	
				x	y
EQ1: MANJIL, IRAN 1990 p Stn: BHRC Station	7.4	50	Strike-Slip	0.13	0.18
EQ2: LANDERS 1992 c Stn: Palm Springs - Airport	7.4	41.9	Strike-Slip	0.08	0.09
EQ3: KOCAELI, TURKEY 1999 p Stn: Arcelik	7.5	10.6	Strike-Slip	0.22	0.15
EQ4: HECTOR MINE 1999 c Stn: Joshua Tree Fire Station	7.1	51.5	Strike-Slip	0.15	0.19
EQ5: BORREGO MOUNTAIN 1968 c	6.8	34.7	Strike-Slip	0.13	0.06
EQ6: CHICHI 1999 c Stn: Taichung	7.6	60.9	Reverse Oblique	0.11	0.11

Note: Stn – Station where the ground motion was recorded

A.3 Spectral Matching

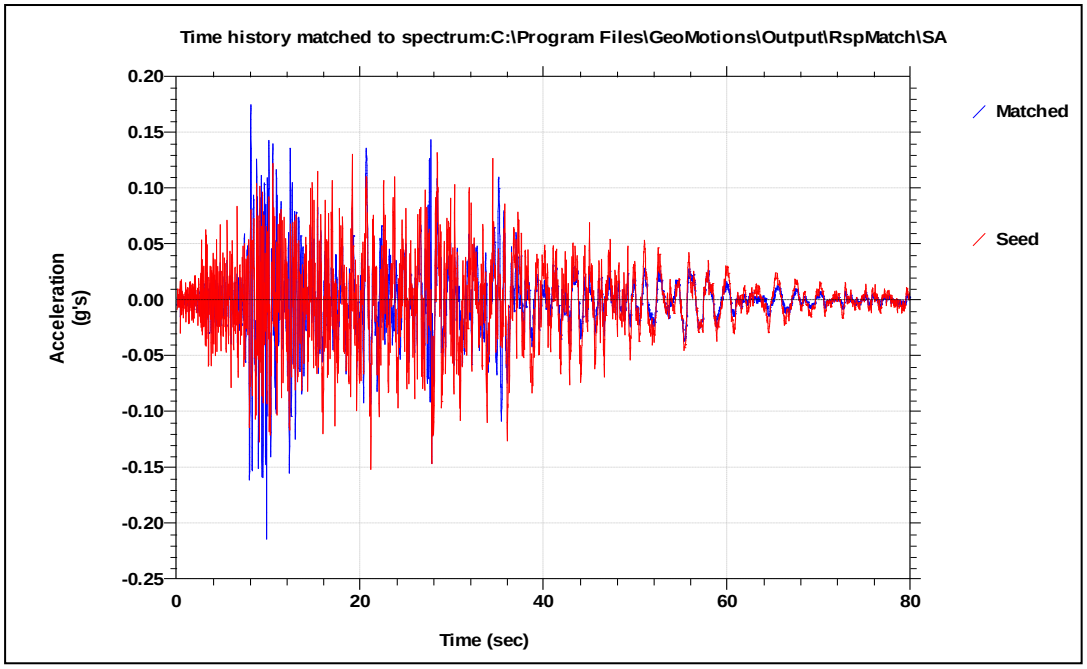

Figure A4. Spectrally-matched time history for one of the selected earthquakes

Appendix B: Ground Response Analysis in DEEPSOIL v5.1

B.1 Porewater Pressure Profiles for Banadero, Calamba

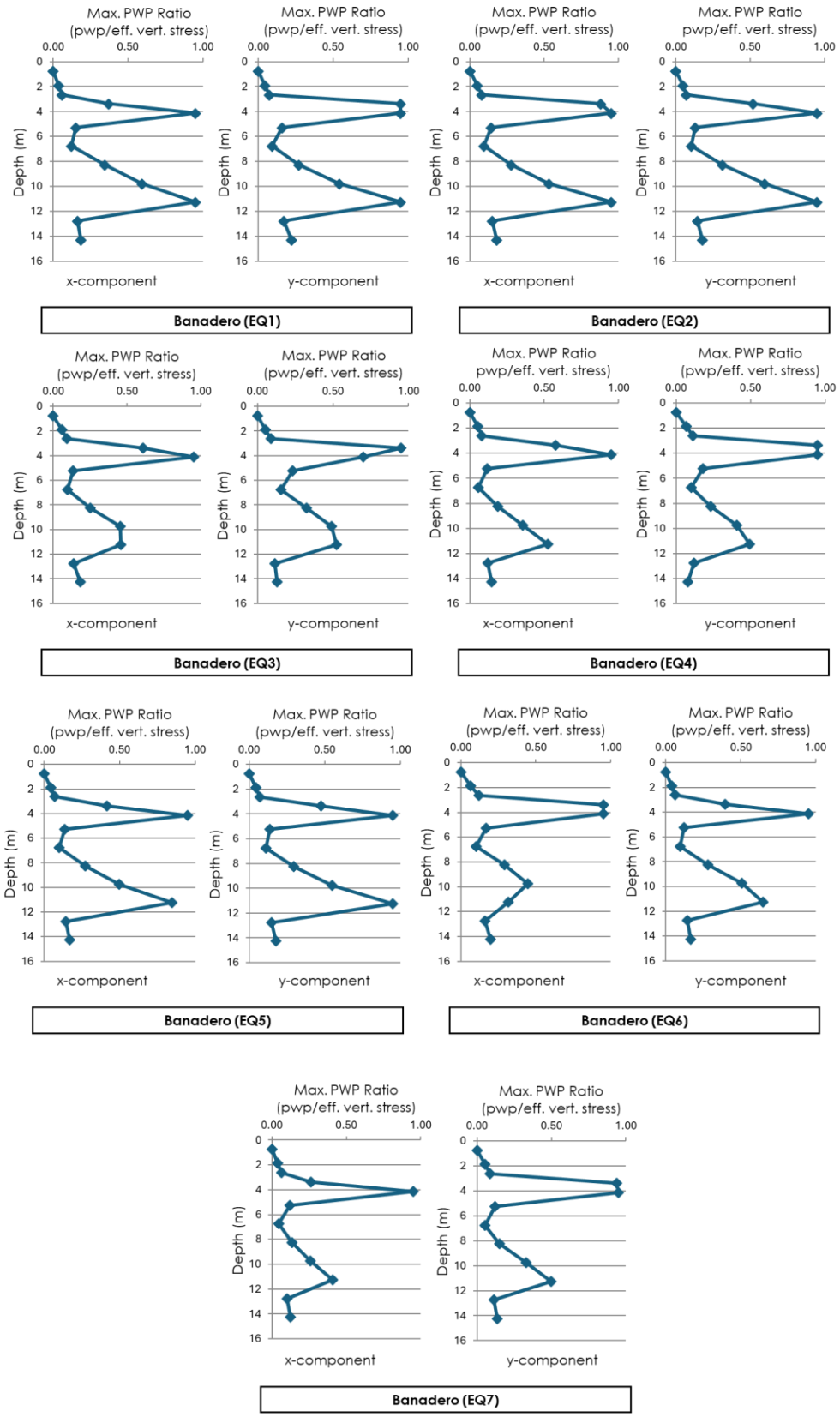

Figure B1. Porewater pressure profiles for Banadero, Calamba using seven (7) earthquakes in x- and y- components.

B.2 Porewater Pressure Profiles for Banay-Banau, Cabuyao

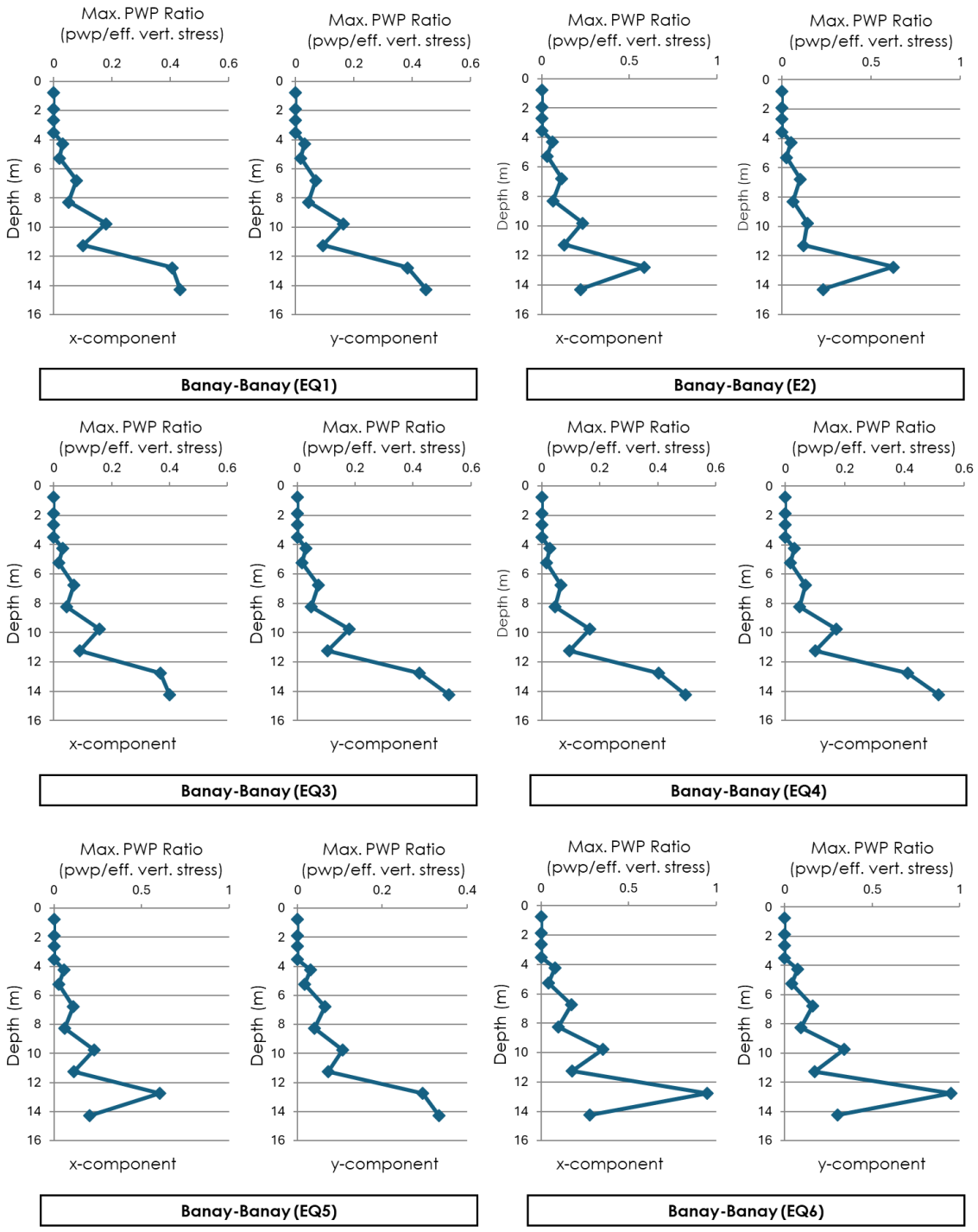

Figure B2. Porewater pressure profiles for Banay-Banay, Cabuyao, using six (6) earthquakes in x- and y- components.